

# Characterization of Turbulence Generated by an Active Grid with Individually Controllable Paddles

T. Skeledzic, J. Krauss, H. Lienhart, Ö. Ertunc and J. Jovanovic

**Abstract** An active grid with individually controllable paddles was constructed to generate strong turbulence ( $Re_\lambda > 200$ ). Measurements of turbulence quantities using the hot-wire technique were conducted in a wind tunnel along the flow on the centre line and on an off-centred line in the wake of this grid. The effect of two different motion sequences of the active grid paddles as well as the influence of the clock rate of the paddles were tested. Finally, measurements with a fixed paddle angle were carried out. The results confirmed that the active grid is suitable to generate the intended strong turbulence. Maximum  $Re_\lambda$  was obtained when the uniform probability density distribution was used. Turbulence generated with fixed paddle angle still delivered turbulence with  $Re_\lambda \sim 100$ .

## 1 Introduction

Turbulent flows in nature (in the atmosphere, oceans and the human body) and in technological applications (combustion chambers, pipe lines, mixers) possess length and velocity scales in a very wide range which are commonly quantified by the turbulence Reynolds number:

$$Re_\lambda = \frac{\sqrt{u^2} \lambda}{\nu}$$

---

T. Skeledzic · J. Krauss · H. Lienhart (✉) · Ö. Ertunc · J. Jovanovic  
Lehrstuhl Für Strömungsmechanik, Friedrich-Alexander Universität Erlangen-Nürnberg,  
Cauerstr. 4, 91058 Erlangen, Germany  
e-mail: hermann.lienhart@fau.de

Ö. Ertunc  
e-mail: ozgur.ertunc@ozyegin.edu.tr

Ö. Ertunc  
Mechanical Engineering Department, Özyeğin University, 34794 Çekmeköy, İstanbul,  
Turkey

based on the Taylor micro scale  $\lambda$ , which is a measure of dissipation length scale, and the energy of turbulence represented by the r.m.s. of the longitudinal fluctuations.  $Re_\lambda$  values of turbulent flows in technological applications start typically at about 200 and can be as high as 1500 [6, 11].

According to Kolmogorov's theory of local isotropy [9, 10], for sufficiently large Reynolds numbers the spectral separation in the flow which measures the strength of the turbulence defined by the ratio between the large and the smallest scales of motion is determined entirely by the amount of energy transferred to the smaller eddies. This energy is dissipated by the latter through the action of viscosity. In that state the motion of the small eddies is weakly related to the motion of the anisotropic and inhomogeneous larger eddies and their motion is nearly isotropic. These ideas were essential in many turbulence models and large eddy simulations since they provide the dynamics of the small scale fluctuations.

Therefore, many experiments have been undertaken with the aim to study the  $Re_\lambda$  range where Kolmogorov's theory is valid. To generate approximately homogeneous isotropic turbulence in a wind tunnel, regular static grids were usually employed. However, these grids could only generate turbulence intensities of a few percent and turbulence Reynolds numbers up to less than 100 [4]. In order to overcome these limitations, so called active grids, as proposed by Makita [12], were developed, to generate turbulence at Reynolds numbers an order of magnitude higher than with their static counterparts. Mydlarski and Warhaft [13], Kang et al. [8] and Celik and van de Water [3] used similar grids to study large-scale turbulent flows at turbulence Reynolds numbers of several hundreds. Mydlarski and Warhaft [13] showed that the inertial range of the velocity spectrum develops with increasing  $Re_\lambda$  and that turbulence with  $Re_\lambda > 200$  (strong turbulence) is qualitatively different from turbulence with  $Re_\lambda < 100$  (weak turbulence). More recently, Bewley et al. [2] utilized a refined active grid layout with independently rotating paddles allowing the anisotropy of the generated turbulence to be controlled, Griffin et al. [7].

A very similar approach was adopted for the present active grid design which used dedicated servo motors for each paddle to permit individual control with the aim to generate strong turbulence at large turbulence Reynolds numbers ( $Re_\lambda > 200$ ) under well-controlled conditions. The grid was installed and tested in the wind tunnel of the Lehrstuhl für Strömungsmechanik (LSTM) at Friedrich-Alexander-Universität Erlangen-Nürnberg. Experiments were conducted to quantify the turbulence generated and to investigate the effect of different motion sequences of the grid.

## 2 Experimental Setup and Data Processing

### 2.1 Wind Tunnel and Measuring Technique

The experiments were performed in the wind tunnel at LSTM. This facility is a closed-loop type low-speed wind tunnel with a  $1.87 \times 1.4 \text{ m}^2$  open test section

and a maximum speed of 60 m/s. The cross-sectional area of the test section of the wind tunnel is much larger than that of the active grid to be tested. So the active grid was mounted inside a specific closed test section insert positioned in the open test section of the wind tunnel. The wind tunnel was operated in a control loop mode in order to keep the mean velocity constant at about 4.5 m/s behind the active grid in all test runs.

Figure 1 shows a sketch of the test set-up with the test section insert inside the wind tunnel test section, the active grid and the hot-wire probe mounted on a 3D traversing system which allowed the probe to be positioned at any arbitrary position close to the central plane of the wake flow behind the active grid. The coordinate system applied for the study is also shown in the sketch.

To conduct the measurements of the turbulent velocity fluctuations, a DANTEC StreamLine constant temperature hot-wire anemometer (CTA) was employed. A single normal wire (SN-wire probe, 55P11) with a diameter of 5  $\mu\text{m}$  was used for all the measurements. In order to minimize the electronic noise, the amplifier filter and the amplifier gain in the feedback loop of the CTA were set to minimum. The output signal of the anemometer was filtered by an integrated 3rd order Butterworth low pass filter with an upper frequency limit set at 3 kHz. From the filtered hot wire signal the DC offset was subtracted and the AC content was amplified to match the input sensitivity of the 16-bit A/D converter (NI USB 6259) which acquired the data at a sampling rate of 6 kHz. It turned out that at measuring positions very close behind the active grid the turbulence intensity generated significantly exceeded 20% which is considered as the upper limit for reliable hot-wire measurements, but most of the data lay well below 15%. For further studies X- and triple-wire probes or laser-Doppler velocimetry will be employed.

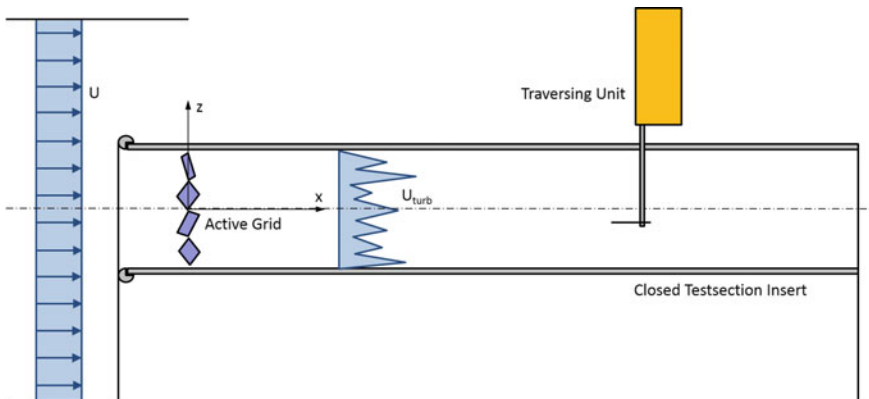


Fig. 1. Test set-up with test section insert in LSTM wind tunnel

## 2.2 Active Grid

The active grid will later be installed in the Refractive Index Matched Tunnel (RIMT) at LSTM which uses a cosmetic white oil as the test fluid whose kinematic viscosity is very similar to that of air. Therefore, the size and the construction of the active grid were adapted to its final use. It spans a cross-section of  $600 \times 450 \text{ mm}^2$  and its components were made from stainless steel. The cross-section was covered by 24 paddles arranged in 6 columns and 4 rows with axes of rotation positioned under  $45^\circ$  in an alternating orientation. Each paddle could be controlled individually by its own servo motor, which gives additional degrees of freedom in the possible patterns of paddle movement. Each of the 24 independent actuators can give a rotation of maximal  $90^\circ$  between fully open and fully closed cross-section. However, the geometry of the paddles was designed in such a way that at the fully closed position the tunnel is not blocked completely due to circular openings and spacing between the paddles. These openings also initiate smaller scales of turbulent fluctuations and in this way promote the generation of an equilibrium spectrum of scales in the turbulence cascade. A photograph of the active grid and the setup in the closed test section insert are shown in Fig. 2.

The 24 servo motors were controlled by a real time FPGA (Field Programmable Gate Array) system installed inside the tunnel. Motion parameters were delivered to the FPGA by WLAN so that only power cables had to pass into the tunnel, thereby minimizing leakage problems. A sketch of the control electronics can be found in Fig. 3.

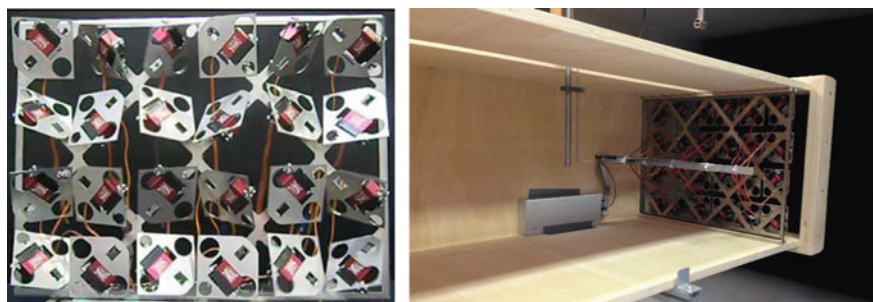
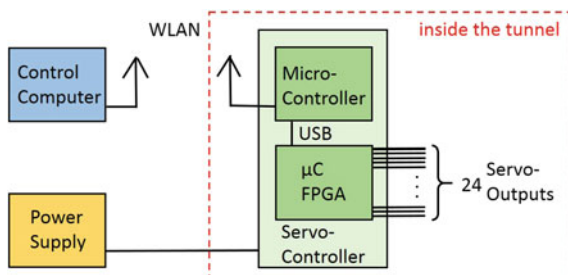


Fig. 2. Active grid on *left* side, test section setup on *right* side

Fig. 3. Block diagram of control electronics



The interior of the test section insert was made accessible for the traversing unit through a slot in the top lid which was covered where not needed. The development of the turbulence behind the active grid was monitored by hot-wire measurements along the centre line and along a parallel line one quarter of the grid height below the centre line of the test section. Measurements were made in 8 downstream positions beginning from 0.4 m behind the grid to 2.0 m (corresponding to approximately 4–20 mesh sizes of the grid) in steps of 0.2 m.

### 2.3 Data Processing

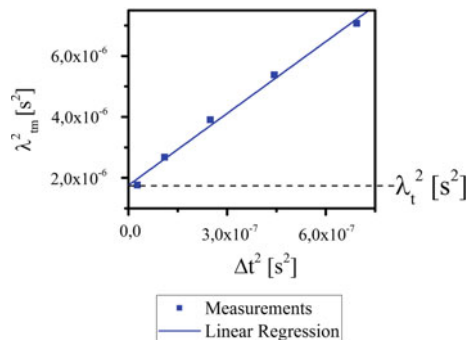
In order to characterize the performance of the different paddle motion sequences statistical quantities were derived from the measured velocity time traces. Besides mean value, standard deviation and their dimensionless quotient  $Tu$  emphasis was placed on the integral time scale  $L_t$  and the Taylor micro time scale  $\lambda_t$  of the velocity fluctuations. The integral time scale was derived from integrating the auto-correlation function. To compute velocity derivatives and Taylor microscale the method of Aronson and Löfdahl [1] was adopted. Using the frozen flow hypothesis, the measured micro time scale  $\lambda_{tm}$  derived at different time increments  $\Delta t$  can be developed in a Taylor series in the following way

$$\left(\frac{\lambda_{tm}}{\lambda_t}\right)^2 = 1 + c\left(\frac{\Delta t}{\lambda_t}\right)^2 \quad \text{where} \quad \lambda_{tm}^2 = \frac{\overline{u^2}}{\left(\frac{u(t+\Delta t) - u(t)}{\Delta t}\right)^2}.$$

Plotting  $\lambda_{tm}^2$  over  $\Delta t^2$  and extrapolating the linear fit regression to the ordinate resulted in the square of the Taylor micro time scale  $\lambda_t$ , Fig. 4. The Taylor micro length scale  $\lambda$  needed to compute the turbulence Reynolds number  $Re_\lambda$  was then computed using the frozen flow hypothesis.

In preliminary tests it turned out that the integral time scales were on the order of 0.04 s in the turbulent wake flow. Choosing a sampling time of 60 s per measuring position therefore corresponded to about 1500 integral time scales. At a sampling frequency of 6 kHz this meant 360,000 data points per measuring position.

**Fig. 4.** Example of the determination of micro scale  $\lambda_t$  according to Aronson and Löfdahl [1]



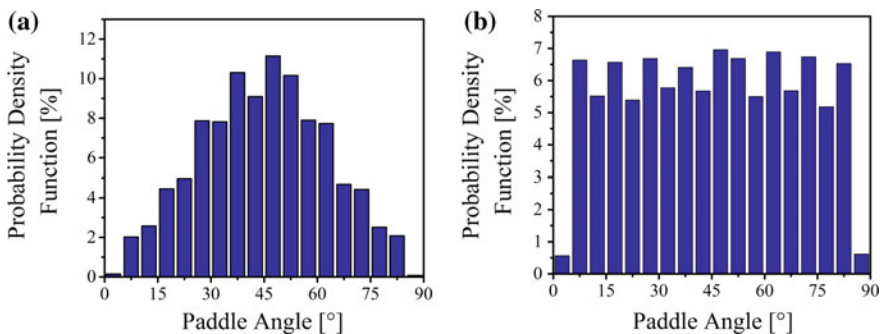
### 3 Results and Discussions

The experiments focused on the measurement of statistical quantities of the fluctuating velocity while using different motion sequences of the servo motors. To this end, two different motion sequences were developed and applied at two different clock rates. Both sequences set random angular positions of the paddles, the first one for a Gaussian probability density distribution (random Gaussian) and the second for a uniform distribution (random uniform), see Fig. 5. In both cases the mean paddle angle was  $45^\circ$ .

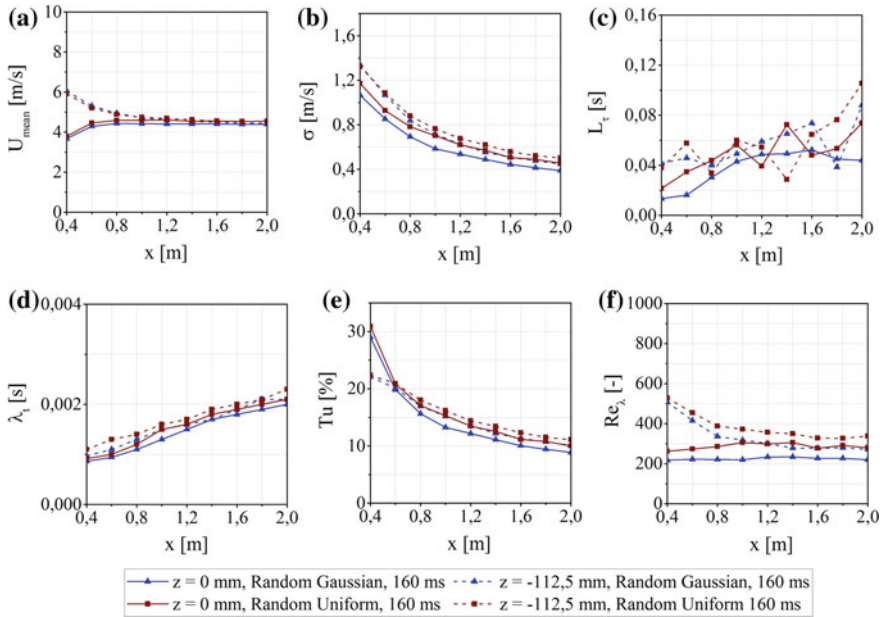
The clock rate set the time period (160 ms or 80 ms, respectively) at which the paddles were set to a new angular position.

Figure 6 compares the results for random Gaussian and random uniform distribution motion sequences; the clock rate in these tests was set at 160 ms. Both cases show quite large differences in the measured mean velocities on centre line and off centre between 0.4 and 1.0 m behind the active grid; further downstream the mean velocities almost converged. This indicates that the mean velocity field from this point on (approximately 10 grid sizes) is approximately independent of crosswise position. A similar behaviour can be seen in the development of the turbulence intensity  $Tu$  but the values already converged 0.5 m behind the grid, hence faster than the mean. The generated turbulence decayed with increasing distance from the grid. Both the integral time scale and the Taylor micro scale were increasing at downstream positions, as expected [5]. The turbulence Reynolds number  $Re_\lambda$  showed an almost constant behaviour on the centre line of about 220 or 290, respectively, the higher value referring to random uniform motion sequence. Off centre it started at significant higher values and decreased downstream.

Figures 7 and 8 compare the results for the two clock rates (160 and 80 ms) and the two motion sequences (random Gaussian and random uniform) respectively. As can be seen from the graphs, an increase of the clock rate did not influence the statistical quantities significantly in either case. On the contrary, the results of the two test runs almost coincided with each other. Increasing the clock rate did not



**Fig. 5.** Probability density functions of the paddle motion sequences, random Gaussian (a), random uniform (b)



**Fig. 6.** Development of mean velocity (a), standard deviation (b), integral time scale (c), Taylor microscale (d), turbulence intensity (e) and turbulence Reynolds number (f) measured on centre line and off centre with a random Gaussian and a random uniform motion sequence at a clock rate of 160 ms

increase either the turbulence intensity or the turbulence Reynolds number. Comparing Figs. 7 and 8 with Fig. 6 reveals that all the plotted quantities behaved quite similarly but generally the random uniform motion sequence led to higher turbulence Reynolds numbers compared to the random Gaussian motion sequence.

In addition to the measurements with actively moving paddles, the development of the statistical quantities with the paddles fixed at  $30^\circ$  was investigated, see Fig. 9. Since there was no movement during the test runs no additional energy was required. This type of stationary 3D grid obviously caused a higher pressure loss compared to the former tests, as indicated by the decreases of mean velocity behind the grid. While the microscale was only marginally changed, the turbulence intensity as well as the integral length scale were noticeably lower than for the active grid. Therefore, it was the lower turbulence intensity, not the changes in the microscale, that resulted in reduced values for turbulence Reynolds number. Nevertheless, this type of a stationary 3D grid showed an interesting performance compared to normal grids. While it did not reach the performance of the active grid its construction would be much less complicated and expensive.

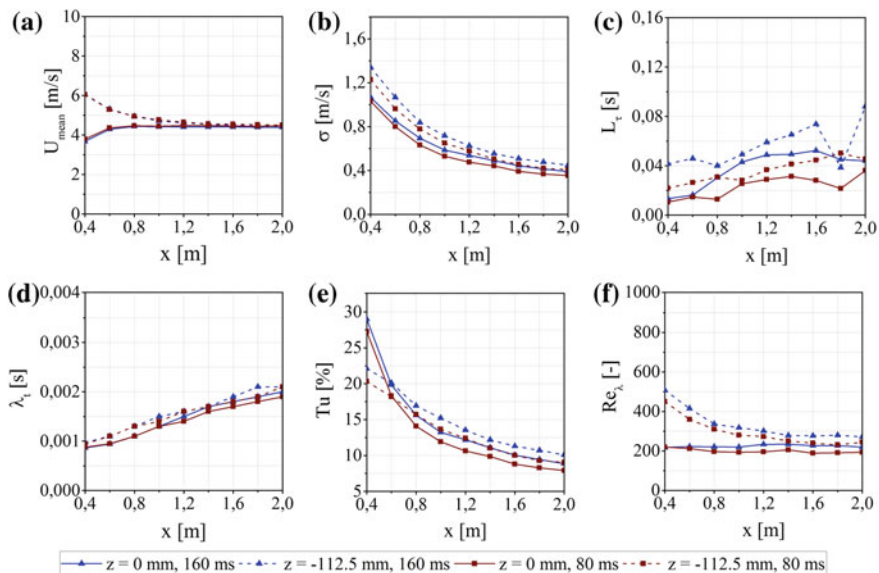


**Fig. 7.** Development of mean velocity (a), standard deviation (b), integral time scale (c), Taylor microscale (d), turbulence intensity (e) and turbulence Reynolds number (f) measured on centre line and off centre with a random Gaussian motion sequence and a clock rate of 160 and 80 ms

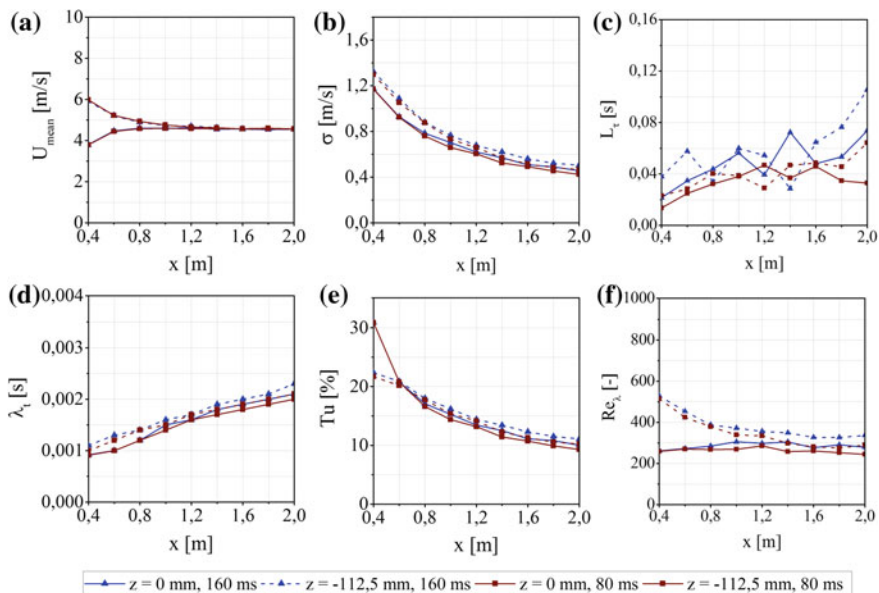


**Fig. 8.** Development of mean velocity (a), standard deviation (b), integral time scale (c), Taylor microscale (d), turbulence intensity (e) and turbulence Reynolds number (f) measured on centre line and off centre with a random uniform motion sequence and a clock rate of 160 and 80 ms



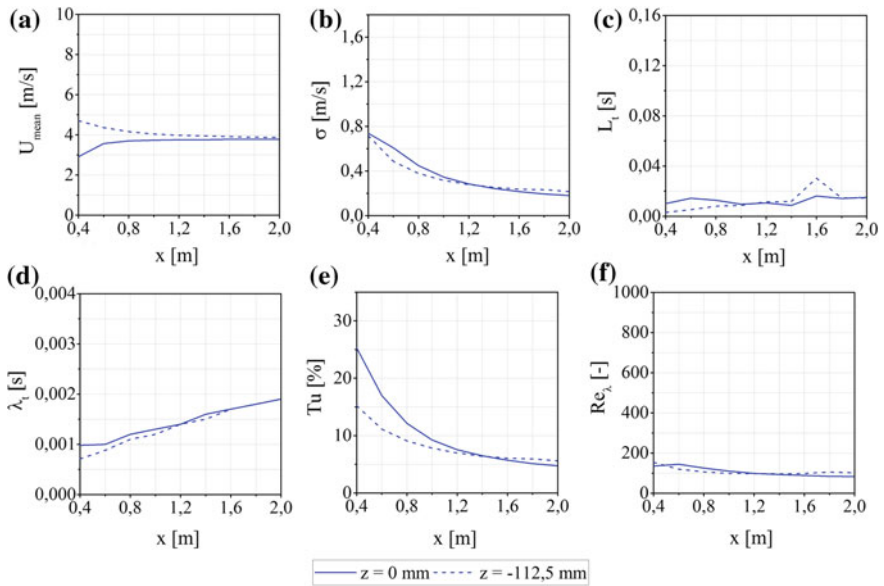


**Fig. 9.** Development of mean velocity (a), standard deviation (b), integral time scale (c), Taylor microscale (d), turbulence intensity (e) and turbulence Reynolds number (f) measured on centre line and off centre with the paddles stationary at  $30^\circ$

## 4 Conclusions

An experimental study has been carried out to investigate the influence of different motion sequences of an active grid on the generated turbulence in the wake flow. The aim was to generate high turbulence intensities, large turbulence Reynolds numbers and large integral length scales. The presented results show that the use of an active grid with individually controllable paddles increased the turbulence intensity as well as the turbulence Reynolds number considerably in comparison to conventional passive grid generated turbulence [5]. The grid was found to be capable of generating turbulence with intensities exceeding 20%, integral time scales up to 0.1 s and turbulence Reynolds numbers up to 520. The best results were achieved using a random motion sequence with uniform probability density distribution and they were almost independent of the clock rate.

**Acknowledgements** Authors acknowledge the financial support given by EU within the EUHIT project.

## References

1. Aronson, D., Löfdahl, L.: The plane wake of a cylinder: measurements and inferences on turbulence modelling. *Phys. Fluids* **A5**(6), 1433–1437 (1993)
2. Bewley, G.P., Kassel, J., Bodenschatz, E.: Control of turbulence with a high degree-of-freedom active grid. In: 14th European Turbulence Conference (2013)
3. Cekli, H.E., Van de Water, W.: Tailoring turbulence with an active grid. *Exp. Fluids* **49**, 409–416 (2010)
4. Comte-Bellot, G., Corrsin, S.: Simple Eulerian time correlation of full- and narrow-band velocity signals in grid-generated “isotropic” turbulence. *J. Fluid Mech.* **48**, 273–337 (1971)
5. Ertunc, Ö.: Experimental and numerical investigations of axisymmetric turbulence. In: PhD Thesis, Universität Erlangen-Nürnberg, Lehrstuhl für Strömungsmechanik (2007)
6. Friehe, C.A., VanAtta, C.W., Gibson, C.H.: Jet turbulence: dissipation rate measurements and correlations. In: AGARD Conference Proceedings 93 (1972)
7. Griffin, K., Wie, N., Hultmark, M., Bodenschatz, E., Bewley, G.P.: Correlated forcing with an active grid to control turbulence. XXIV ICTAM Montreal (2016)
8. Kang, H.S., Chester, S., Meneveau, C.: Decaying turbulence in an active—grid-generated flow and comparison with large-eddy simulation. *J. Fluid Mech.* **480**, 129–160 (2003)
9. Kolmogorov, A.N.: Equations of turbulent motion in an incompressible fluid. *Izv. Akad. Nauk. SSSR Serr. Fiz.* **6**, 56–58 (Imperial College Report No. N/6–1968) (1942)
10. Kolmogorov, A.N.: A refinement of previous hypotheses concerning the local structure of turbulence in a viscous incompressible fluid at high reynolds number. *J. Fluid Mech.* **13**, 82–85 (1962)
11. Larssen, J.V.: Large scale homogeneous turbulence and interactions with a flat-plate cascade. In: PhD Thesis, Virginia Polytechnic Institute and State University (2005)
12. Makita, H.: Realization of a large-scale turbulence field in a small wind tunnel. *Fluid Dyn. Res.* **8**, 53–64 (1991)
13. Mydlarski, L., Warhaft, Z.: On the onset of high-reynolds-number grid-generated wind tunnel turbulence. *J. Fluid Mech.* **320**, 331–368 (1996)